Notes

Toughening of Artificial Silk by Incorporation of Carbon Nanotubes

David Blond, Denis N. McCarthy, Werner J. Blau, and Jonathan N. Coleman*

School of Physics, Trinity College Dublin, Dublin 2, Ireland

Received August 31, 2007
Revised Manuscript Received October 12, 2007

Introduction

Even in the twenty-first century, spider silk remains one of the most impressive structural materials. The product of 400 million years of evolution, spider silk is produced in a variety of forms, each extremely well adapted to the task for which it has been developed. For example, spider dragline silks display values of Young's modulus, strength and toughness (10 GPa, ~1 GPa, and 123 J/g, respectively), perfectly suited for use as web frames, guy lines, or tethers.[1] In contrast, viscid silks of the types used in the web spirals are strong and tough but extremely compliant, ideal for catching insects.[2] While spider silk would be perfect for a range of commercial and medical applications, native silk cannot be harvested due to our failure to domesticate spiders. Silkworm silk has traditionally been used as a substitute. However, its mechanical properties are generally inferior to spider silk.[2] Recently, a major breakthrough has been made with the demonstration of the production of silk via protein synthesis in mammalian cells.[3] This product, selling under the name of Biosteel, can be dissolved and coagulation spun into the fibers, which, when post-treated, display mechanical properties similar to natural spider dragline silk.[3]

Progress toward strong, tough fibers has also been made by embedding carbon nanotubes in polymer matrices. Nanotubes are hollow nanoscale carbon cylinders that display immense strength (~60 GPa) and stiffness (~1 TPa).[4] Coupled with their large aspect ratio, these mechanical properties make nanotubes ideal fillers for reinforcing polymers.[5] By coagulation spinning fibers from polymer-nanotube composite dispersions, materials with strength of ~1 GPa and toughness approaching 1000 J/g have been demonstrated.[6,7]

These nanotube-based composite fibers share much in common with spider silk. The mechanisms behind the superlative mechanical properties are similar in both cases. In nanotube-based composites, stress is transferred from polymer matrix to nanotube. This, coupled with extensive reorganization of the matrix at high applied stress, results in high toughness. In silks, the same mechanisms apply with protein crystallites playing the role of the nanotubes and disordered regions acting as the matrix.[1]

With this in mind, it seems obvious to attempt to incorporate nanotubes into a silk-like material. For the silk-like material, we chose the synthetic spider silk, Biosteel. Functionalized nanotubes were chosen, with the nature of the functionality determined by the requirement that both nanotubes and Biosteel be soluble in the same solvent. We produced composite films based on Biosteel, with a range of nanotube mass fractions by solution processing and drop casting. These films were then investigated using tensile measurement to assess potential mechanical reinforcement.

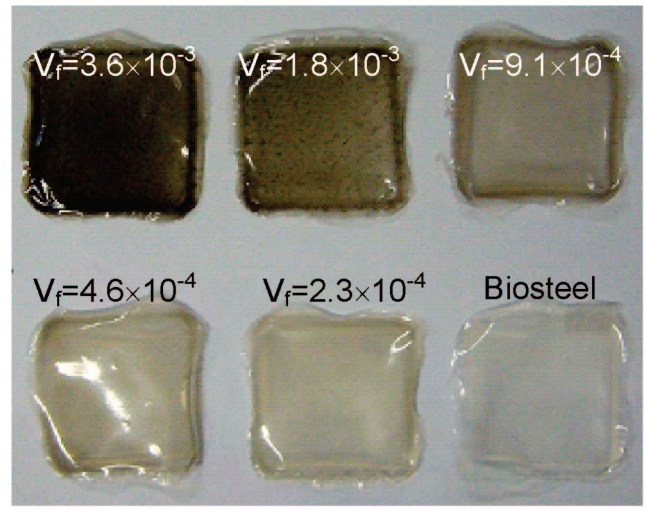

Figure 1. Drop-cast biosteel composite films, with a range of volume fraction of nanotubes from 0 to 3.6 × 10^{-3}.

Experimental Section

For this study, composites were prepared using Biosteel powder[3] purchased from Nexia Biotechnologies Inc. (www.nexiabiotech.com), and SWNTs functionalized with octadecylamine were purchased from Carbon Solutions Inc. (www.carbonsolution.com). First, Biosteel powder was dispersed at a concentration of 30 g L^{-1} in 1,1,1,3,3,3-hexafluoro-2-propanol using a high power sonic tip (120 W, 60 kHz) for 2 min followed by a mild sonication in a sonic bath for two hours. Then SWNTs were added at a mass fraction of 0.5 wt % of the Biosteel mass and dispersed using an extra two minutes of high powder sonic tip followed by two hours in a sonic bath. Afterward, this primary solution was blended with a solution of Biosteel at 30 g L^{-1} to produce a range of mass fraction down to 0.031 wt %. After blending, an extra sonication process was carried out on each sample with high power sonic tip and sonic bath using the same time treatment as before. A photograph of the range of dispersions, as well as optical micrographs of thin liquid films deposited from each dispersion, are shown in Figure S1. A small number of micron-sized aggregates are observed in the 0.031 wt % dispersion. By analogy with other types of nanotube dispersions, we believe these aggregates coexist with a large population of well-dispersed nanotubes.[8,9] As the nanotube content increases, the number and size of these aggregates increases. However, these aggregates are stable against subsequent aggregation and sedimentation. Dispersions stored for up to four months have not displayed any coarsening over that time.

Free-standing films were fabricated by dropping 1.5 mL of each solution onto a polished Teflon square that was placed in a vacuum oven for 24 h to allow the evaporation of the solvent. This procedure was repeated three times in order to obtain an average film thickness of 75 μm (Figure 1). The films were then peeled from the substrate and cut into strips of 10 mm × 2.5 mm × 75 μm. The width and thickness of each strip were measured using a low torque digital

* Corresponding author. E-mail: colemaj@tcd.ie.

10.1021/bm700971g CCC: $37.00
Published on Web 11/22/2007

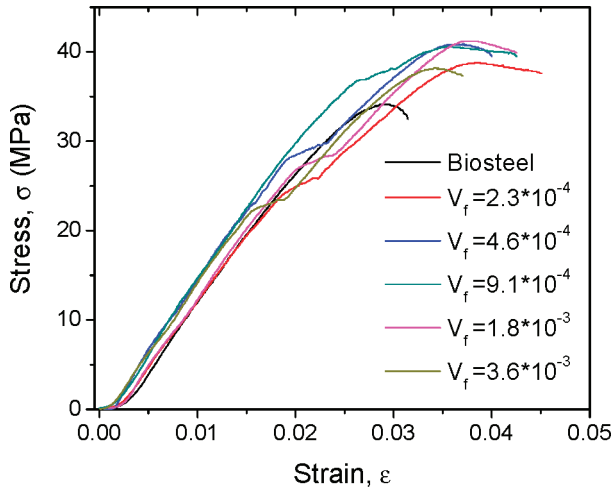

Figure 2. Representative stress–strain curves for Biosteel-based composite for a range of nanotube volume fractions.

micrometer. For each sample, nanotube mass fractions were converted into volume fraction, V_f, using densities of 1500 kg/m^3 and 1100 kg/m^3 for nanotubes and Biosteel, respectively. Mechanical tests were performed using a Zwick tensile tester Z100 using a 100 N load cell with a cross-head speed of 1 mm min^{-1}. For each volume fraction, stress–strain measurements were made on five strips. From each set of five curves, the Young's modulus (Y), tensile strength (σ_C), strain at break (ϵ_B), and toughness (T) were measured, and the mean and standard error were calculated.

Results and Discussion

Photographs of the films are shown in Figure 1. Biosteel appears as a transparent film. Addition of small amounts of nanotubes resulted in a darkening of the film without any loss of uniformity. However, above a volume fraction of 1.8×10^{-3}, small nanotube aggregates are clearly visible. These aggregates may have nucleated from the very small aggregates observed in the dispersions. However, at these volume fractions, even perfectly dispersed nanotubes might be expected to display some aggregation on drying. At a volume fraction of 1.8×10^{-3}, the average nanotube center to center distance within the film is ~75 nm. As the nanotubes used here are ~1 μm long, it is not surprising that internanotube contact may result during the drying phase, resulting in aggregation in higher volume fraction films.

Tensile measurements were carried out to determine the mechanical properties of the Biosteel and composite films. Shown in Figure 2 are representative stress–strain curves for the materials studied in this work. The strain, ϵ, represents the fractional elongation, while the stress, σ, is the applied force divided by the cross sectional area of the unloaded sample.

The Biosteel films display elastic behavior up to strains of ~2.5% before deforming plastically up to fracture at ~3.1%. The Young's modulus, strength, and toughness of the Biosteel films were 1.6 GPa, 36.5 MPa, and 1.7 J/g, respectively, similar to regenerated *Bombyx mori* silk fibers.[10] These values are significantly larger than those previously observed for as-prepared, coagulation-spun Biosteel fibers (<1.3 GPa, <2.3 MPa, <1 J/g, respectively).[3] However, it should be pointed out that these fibers demonstrated dramatically improved properties[3] after postspinning drawing, reaching moduli and strengths of 4–10 GPa and 160–200 MPa, respectively. Such coagulation spun fibers also exhibited plastic deformation up to 130% strain and so possessed extremely large T values of 50–80 J/g. In comparison, natural silk produced in the major ampullate (MA) gland of the spider *Araneus diadematus* displays stiffness, strength, and T of 10 GPa, 1.1 GPa, and ~140 J/g^2. These impressive values are due to the presence of alanine-rich crystalline domains that act to reinforce all natural silks.[1,2,11] It is known that postdrawing of regenerated silks, especially in the presence of water, results in the reorganization of the protein secondary structure, increasing the crystalline fraction and improving the mechanical properties.[11] Dissolution of proteins in strong denaturing solvents, such as 1,1,1,3,3,3-hexafluoro-2-propanol (as used here), is known to disrupt the secondary structure, resulting in a low-crystalline fraction.[3,11] Thus, the mechanical properties observed for the Biosteel films produced in this work are consistent with silk-like materials with high amorphous content. Interestingly, our mechanical properties are better than lightly drawn regenerated spider silk (*Nephilia clavipes*, MA gland).[11]

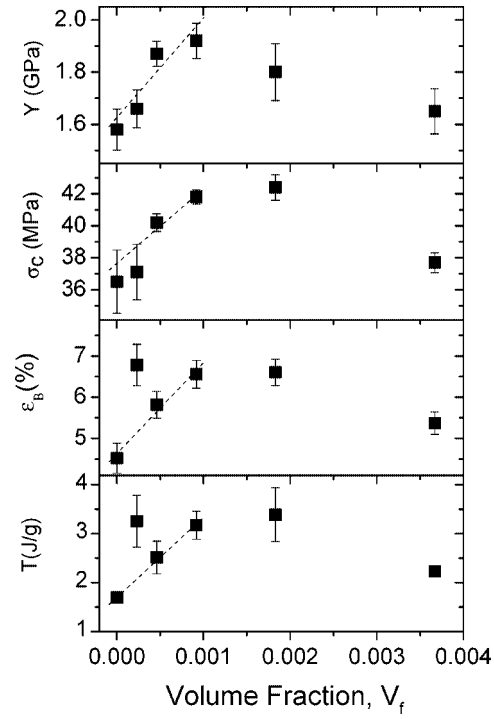

Figure 3. Young's modulus, ultimate tensile strength, strain to break, and toughness of the composites for various volume fractions of nanotubes.

The composite samples display broadly similar stress–strain curves to the pure Biosteel. However, adding small amounts of nanotubes results in significant improvements in the four main mechanical parameters: Y, σ_C, T, ϵ_B. The means and standard errors of all four quantities are shown as a function of nanotube volume fraction in Figure 3. At low volume fractions, all four parameters increase linearly up to an optimum volume fraction of ~10^{-3}, followed by a decrease in all parameters at higher nanotube contents. This optimal volume fraction is consistent with the maximum aggregate free volume fraction (Figure 1). The reduction in all mechanical properties above this concentration underlines the importance of nanotube dispersion for mechanical reinforcement.[5]

The Y increases linearly with volume fraction, as predicted by the rule of mixtures,[12,13] reaching 1.9 GPa at the optimum loading level. The rate of increase (dY/dV_f) was found to be 380 ± 100 GPa. The rule of mixtures predicts dY/dV_f to be given by

Table 1. Mechanical Properties of the Materials Studied in this Work

	dY/dV_f (GPa)	$d\sigma_C/dV_f$ (GPa)	dT/dV_f J/g	$d\epsilon_b/dV_f$
value	381 ± 105	4.65 ± 1.26	1640 ± 288	22 ± 5.4
increase	21.5%, 1.58 GPa → 1.92 GPa	14.5%, 36.5 MPa → 41.8 MPa	87%, 1.69 J/g → 3.17 J/g	45%, 0.045% → 0.065%
saturation point (V_f)	9.1×10^{-4}	9.1×10^{-4}	9.1×10^{-4}	9.1×10^{-4}

$$\frac{dY}{dV_f} = \eta_0 Y_{eff} - Y_b \approx \eta_0 Y_{eff} \quad (1)$$

where Y, Y_{eff}, and Y_b are the composite modulus, the effective nanotube modulus,[5,12] and the Biosteel modulus, respectively. η_0 is the fiber orientation efficiency factor, which can be approximated to 0.38 for nanotubes aligned in-plane.[14] The approximation holds when $Y_{eff} >> Y_b$, as is expected to be the case.

For arc discharged SWNTs, such as those used in this study, the maximum value of Y_{eff} is approximately 1 TPa.[4,15] Using eq 1, we can calculate the maximum value of dY/dV_f to be ~380 GPa. This value is identical to the experimental value, indicating that the stress transferred to the nanotubes is maximized over a significant fraction of their lengths.[5] For micron-length nanotubes, this can only happen if the interfacial shear strength is very large, evidence of the effectiveness of the functional groups at transferring stress from the matrix to the nanotube. Ayutsede et al.[16] also made composite fibers by using *Bombyx mori* silk and SWNTs. By adding 1 wt % of unfunctionalized SWNTs, they improved the Y from 312 to 705 MPa, equivalent to $dY/dV_f = 44.6$ GPa. That their value is much lower than the value of $dY/dV_f = 380$ GPa measured in this work is further evidence of the value of attaching appropriate functional groups to any potential mechanical filler material.

The ultimate tensile strength increased linearly with volume fraction from 36.5 MPa (Biosteel) up to 41.8 MPa at a volume fraction of 9.1×10^{-4}. This corresponds to a rate of increase of $d\sigma_c/dV_f = 4.7 \pm 1.3$ GPa. This value is smaller than expected as the maximum possible value of $d\sigma_c/dV_f$ is close to the nanotube strength, that is, ~50 GPa.[5] It is not clear what the reason for this discrepancy is.

The average breaking strain of Biosteel films was 4.5%. While this value is low compared to silks in general[2] and treated Biosteel fibers in particular,[3] this brittleness is not unexpected. Regenerated spider silk fibers prepared in the absence of any water have been observed to be brittle, breaking at strains of 4–8%.[11] What is surprising is the fact that the addition of a volume fraction of 9.1×10^{-4} nanotubes resulted in an increase in the average strain at break from 4.5% to 6.5%. This is unexpected, as addition of nanotubes to a polymer generally reduces the ductility.[5] However, this increase in ductility, coupled with the strength increases translates into an increase in the fiber toughness. The T increased linearly from 1.7 J/g for the Biosteel up to 3.17 J/g for the $V_f = 1.8 \times 10^{-3}$ sample. This is a dramatic increase for a very small content of nanotubes. Previous work by Ayutsede, showed a dramatic drop in T from ~0.5 J/g for a film of electrospun regenerated *Bombyx mori* silk to ~0.02 J/g at a loading level of 0.5%.[16]

It should be pointed out that there are two problems with this work: the mechanical properties saturate at low loading levels and the absence of crystalline protein results in significantly reduced mechanical properties compared to natural silk. The first of these problems could be addressed by careful choice of functional group. The ODA functionalized nanotubes were chosen from a very limited (commercially available) selection on the basis that they could be dispersed in 1,1,1,3,3,3-hexafluoro-2-propanol and so blended with the Biosteel. While cosolubility demonstrates a certain level of compatibly between ODA and Biosteel, we believe that careful choice of functional group could lead to better compatibility, resulting in improved dispersion and less aggregation at high volume fraction. For example, techniques developed to synthesize designed peptides[17] could be modified to functionalize −COOH grafted SWNT, resulting in enhanced SWNT/silk compatibility. In addition, due to alignment effects, it is expected that even higher volume fractions could be attained, without aggregation, in a fiber. Furthermore, due to alignment of nanotube in the fiber, η_0 would be increased to 1. For example, if we could retain dispersion up to 1 vol% (nanotube separation ~10 nm) in a nanotube silk fiber we could expect moduli and strengths of ~12 GPa and ~160 MPa, respectively, even in the absence of protein crystallites.

To address the second problem, we attempted to induce protein crystallization by soaking the films in water followed by wet drawing.[11] After a short period soaking, the films curled up into a quasi-helical shape, indicative of significant internal rearrangement. This, however, made it very difficult to make reproducible mechanical measurements. Another technique tried was to clamp the film in the tensile tester while applying water via a pipette. While this method was not particularly reproducible, strengths of up to 100 MPa were observed. However, no pattern was observed to differentiate the properties of the treated Biosteel from the treated composites. We expect that post-treatment would be much more successful on coagulation-spun composite fibers rather than films. It will be important to determine whether post-treatments, such as drawing in water, result in composite fibers with mechanical properties superior to those previously observed for Biosteel fibers.[3] If this is the case, the result would be a material with truly exciting mechanical properties.

Conclusion

In summary, we have produced nanotube-silk composites by mixing functionalized nanotubes and Biosteel in 1,1,1,3,3,3-hexafluoro-2-propanol. Composite films could be produced by dropcasting from composite dispersions. The mechanical properties of the pure Biosteel films were lower than expected due to the effect of the strong denaturing solvent (Table 1). Increases in stiffness, strength, ductility, and T were observed at very low nanotube loading levels. Analysis of the rate of increase of stiffness with volume fraction show extremely good polymer−nanotube stress transfer. However, all mechanical results saturate at a volume fraction of ~0.1% due to nanotube aggregation. Preliminary experiments showed that the mechanical properties of the films could be further enhanced by postdrawing in the presence of water.

Supporting Information Available. Figure S1 consists of a photograph of the nanotube-Biosteel dispersions and a set of micrographs of thin liquid films deposited from the dispersions. This information is available free of charge via the Internet at http://pubs.acs.org.

References and Notes

(1) Kubik, S. *Angew. Chem. Int. Ed.* **2002**, *41* (15), 2721.

(2) Gosline, J. M.; Guerette, P. A.; Ortlepp, C. S.; Savage, K. N. *J. Exp. Biol.* **1999**, *202* (23), 3295–3303.
(3) Lazaris, A.; Arcidiacono, S.; Huang, Y.; Zhou, J.-F.; Duguay, F.; Chretien, N.; Welsh, E. A.; Soares, J. W.; Karatzas, C. N. *Science* **2002**, *295* (5554), 472–476.
(4) Yu, M. F.; Files, B. S.; Arepalli, S.; Ruoff, R. S. *Phys. Rev. Lett.* **2000**, *84* (24), 5552–5555.
(5) Coleman, J. N.; Khan, U.; Blau, W. J.; Gun'ko, Y. K. *Carbon* **2006**, *44* (9), 1624–1652.
(6) Dalton, A. B.; Collins, S.; Munoz, E.; Razal, J. M.; Ebron, V. H.; Ferraris, J. P.; Coleman, J. N.; Kim, B. G.; Baughman, R. H. *Nature* **2003**, *423* (6941), 703.
(7) Miaudet, P.; Badaire, S.; Maugey, M.; Derre, A.; Pichot, V.; Launois, P.; Poulin, P.; Zakri, C. *Nano Lett.* **2005**, *5* (11), 2212–2215.
(8) Bergin, S. D.; Nicolosi, V.; Giordani, S.; de Gromard, A.; Carpenter, L.; Blau, W. J.; Coleman, J. N. *Nanotechnology* **2007**, *18* (45), 455705.
(9) Giordani, S.; Bergin, S. D.; Nicolosi, V.; Lebedkin, S.; Kappes, M. M.; Blau, W. J.; Coleman, J. N. *J. Phys. Chem. B* **2006**, *110* (32), 15708–15718.
(10) Marsano, E.; Corsini, P.; Arosio, C.; Boschi, A.; Mormino, M.; Freddi, G. *Int. J. Biol. Macromol.* **2005**, *37* (4), 179–188.
(11) Seidel, A.; Liivak, O.; Calve, S.; Adaska, J.; Ji, G. D.; Yang, Z. T.; Grubb, D.; Zax, D. B.; Jelinski, L. W. *Macromolecules* **2000**, *33* (3), 775–780.
(12) Cox, H. L. *Br. J. Appl. Phys.* **1952**, *3* (MAR), 72–79.
(13) Krenchel, H. *Fibre reinforcement*; Akademisk Forlag: Copenhagen, 1964.
(14) Shaffer, M. S. P.; Windle, A. H. *Adv. Mater.* **1999**, *11* (11), 937–941.
(15) Salvetat, J.-P.; Briggs, G. A. D.; Bonard, J.-M.; Bacsa, R. R.; Kulik, A. J.; Stöckli, T.; Burnham, N. A.; Forró, L. *Phys. Rev. Lett.* **1999**, *82* (5), 944.
(16) Ayutsede, J.; Gandhi, M.; Sukigara, S.; Ye, H. H.; Hsu, C. M.; Gogotsi, Y.; Ko, F. *Biomacromolecules* **2006**, *7* (1), 208–214.
(17) Dieckmann, G. R.; Dalton, A. B.; Johnson, P. A.; Razal, J.; Chen, J.; Giordano, G. M.; Munoz, E.; Musselman, I. H.; Baughman, R. H.; Draper, R. K. *J. Am. Chem. Soc.* **2003**, *125* (7), 1770–1777.

BM700971G